www.ijecs.in
International Journal Of Engineering And Computer Science ISSN:2319-7242
Volume – 5 Issue -04 April, 2016 Page No. 16149-16155

Modelling Of Wind Diesel Hybrid System for Reverse Power Management Using Bess.

C.Md.Shareef[1], Rajasekar Thota[2],N Vaseem Raja[3],T.Narasimha Reddy[4]

[1,2,3,4]Assistant Professor vemu institute of technology

ABSTRACT

This paper presents the modeling of a Wind Diesel Hybrid System (WDHS) comprising a Diesel Generator (DG), a Wind Turbine Generator (WTG), the consumer Load, a Ni–Cd Battery based Energy Storage System (BESS) and a Distributed Control System (DCS). All the models of the previously mentioned components are presented and the performance of the WDHS is tested through simulation. Simulation results with graphs for frequency and voltage of the isolated power system, active powers generated/absorbed by the different elements and the battery voltage/current/state of charge are presented for negative load and wind speed steps. The negative load step reduces the load consumed power to a level less than the WTG produced power, so that to balance active powers a negative DG power is needed (DG reverse power). As the DG speed governor cannot control system frequency in a DG reserve power situation, it is shown how the DCS orders the BESS to load artificially the system until the DG power falls in a positive power interval. The negative wind step decreases the WTG produced power, returning the power system to a situation where the needed DG power returns to positive, so that the BESS is not needed to load the system.

1. INTRODUCTION

Power quality and reliability have become a crucial factor for the development of new technologies with the imminent deregulated environment. Distributed generation (DG) systems are expected to play a major role to meet the energy demand with clean environment. DG technologies such as photovoltaic systems, wind turbine, fuel cell, diesel engines are used in various places . Wind energy has received the special attention of researchers in recent times. The advent of power electronic devices have steered a new era of power quality while integrating them with the renewable sources of energy. The renewable systems can either be interfaced with the existing grids or can be operated on a stand-alone basis. Effective capture of wind energy can definitely help to meet the energy needs as is evident in countries such as Germany, Netherlands, Canada etc. Stand alone or isolated systems are common in islands or far rural areas where the utility grid can't reach.

A single renewable energy source may not be able to meet the load demands apart from the fact that continuous supply of energy may not be ensured (say wind is not available on a particular day in a wind farm). This makes the importance of hybrid energy systems such as wind- PV, wind-diesel along with use of battery etc. Owing to the fast controllability and response time of the diesel engines, they are quite popular for integration with wind energy conversion systems (WECS). Hence a wind diesel hybrid system is considered in the thesis. Induction generators are utilized for wind systems. However recent technologies have paved way for other generators such as self-excited type, permanent magnet type etc. which have their relative merits and demerits which has been explored here.

2. THE WDHS ARCHITECTURE AND THE REVERSE POWER SITUATION

The Medium penetration WDHS of Fig.2.1 comprises one DG and one WTG. In DO mode the DG supplies the active and reactive power demanded by the consumer load (in this mode the WTG is shut off so C_T = OFF in Fig. 4.1). The speed governor (speed regulator+ actuator) controlling the DE, performs frequency regulation and voltage regulation is performed by the automatic voltage regulator in the SM.

In WD mode, the WTG also supplies active power and the same regulators as in DO mode are in charge of the frequency and the voltage control (referring to Fig.2.1, C_T = ON in WD mode). The constant speed stall controlled WTG of Fig.2.1 consists of a Wind Turbine (WT) driving an Induction Generator (IG) directly connected to the autonomous grid. In this article a fixed speed no pitch control WTG is used as it has robust construction, low cost and simply maintenance and these are important factors in the remote locations of WDHS, but WDHS with more efficient (and less robust) variable speed WTG consisting of aWT driving a Synchronous generator which is connected to the isolated grid through an electronic double power converter (AC–DC–AC) has also been studied.

As the WTG produced power PT can be greater than the load consumed power P_L, a DL should be incorporated to dump the necessary power to keep the needed DG produced power positive. An Energy Storage System (ESS) can also be used with the same aim as the DL, with the advantage that it is possible to recover later the stored energy. Additionally an ESS can reduce in both DO

and WD modes the needs of spinning reserve and increase the loading to the DGs in order to improve their performance. The addition of an ESS to a large power system can effectively improve system stability and this is more effective in WDHS as they are low inertia isolated power systems where significant frequency deviations occur. The ESSs more used in WDHS are those based on batteries or flywheels. The BESS of Fig.2.1 consists of a battery bank and a power converter which performs the DC/AC conversion to interface the battery bank to the autonomous grid. The BESS is a controlled sink/source of active power. The speed control of the DE of Fig.2.1 is isochronous so the DE will run at constant speed provided that its demanded load is in the range spanning from 0 to its rated power. The diesel speed governor controlling the DE performs the frequency regulation by maintaining an instantaneous balance between the consumed and produced active power. Let us suppose that the BESS is turn off in the WDHS of Fig.2.1, being P_{DE} the mechanical power supplied by the DE, P_T the power supplied by the WTG (also called wind power), PL the power consumed by the load, J and x, the DG inertia and shaft speed respectively, the power equation of the SM is:

$$P_{DE}+P_T-P_L=j\dot{\omega}\frac{d\dot{\omega}}{dt} \qquad (1)$$

Where P_{DE} and P_T are considered positive if produced and P_L is considered positive if consumed. In Eq. (1) the shaft speed x is in rad/s (x = 2pf/p with f the system frequency and the SM pole pairs), no losses are taking into account and it also applies to DO mode where $P_T = 0$, since no WTG is connected. The diesel speed governor will make the DG run at constant speed (dx/dt = 0), so Eq. (1) coverts into Eq. (2) in steady state:

$$P_{DE}+P_T-P_L=0 \qquad (2)$$

To comply with (2), the speed governor sets P_{DE} so that the DE generated power is equal to the net consumed power P_L–P_T. But the diesel speed governor cannot control P_{DE} if P_{DE} is out of the range (0, DE rated power) and the 0 lower limit cannot always be satisfied in a WDHS. The uncontrolled power generated by the WTG (P_T) can be greater than the consumed power by the load (P_L), so to satisfy Eq. (2) the DG power must be negative ($P_{DE} < 0$, DG reverse power). As the speed governor cannot order the DE to consume power, it is unable to regulate frequency. A diesel engine has a temporary small braking capability resulting from engine compression, so it can consume power, but this capability cannot be controlled. On the other hand, if the magnitude of P_L-P_T is greater than the DE braking capability, the system frequency will increase and unless the WTG circuit breaker CT is opened, the power system will collapse as it will be shown in the simulation section. To avoid the reverse power, the WDHS control system must use the controlled sink/source BESS. If the BESS is added to the power system and being P_S the power consumed/supplied by the BESS (it is considered positive if consumed) then Eq. (1) transforms into:

$$P_{DE}+P_T-P_L-P_S=j\dot{\omega}\frac{d\dot{\omega}}{dt} \qquad (3)$$

The WDHS control system must order to the BESS consume active power in order to need a positive P_{DE} to balance active powers in Eq. (3). With $P_{DE} > 0$, the speed governor will resume the control of the system frequency. As it will be shown in the simulation results section, one of the main goals of this article is to show the real time control of the BESS when a reverse power in the DG occurs.

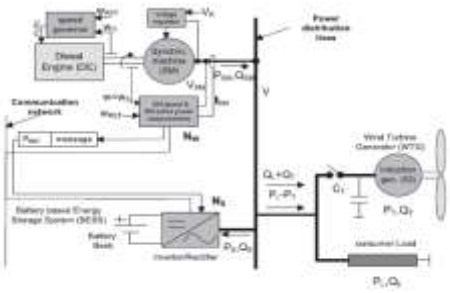

Fig2.1 Layout of the isolated power system + distributed control system considered

3. THE CONTROL SYSTEM AND THE CONTROL ALGORITHM

The proposed control of the BESS in the presented WDHS is by means of a Distributed Control System (DCS). A DCS consists of several CPU based electronic control units (also called nodes) physically distributed and linked by a communication network. As it can be seen in Fig.4.1, the DCS defined consists of two nodes: one sensor node NW, measuring the shaft speed and active power of the SM, and one actuator node: the BESS converter NS. The nodes of a DCS exchang information between them through message passing. The sensor node N_W, depending on its measurements and the WDHS operation mode, calculates the needed reference power P_{REF} to be absorbed/supplied ($P_{REF} > 0$/$P_{REF} < 0$) by the BESS for balancing the active power in the system. P_{REF} is calculated in WD mode by the sum of a proportional plus derivative control applied to the frequency error ef ($e_f = f - f_{NOM}$, where f_{NOM} is the power system rated frequency and f the current system frequency) and the term P_{INV} which prevents the DE reverse power:

$$P_{REF}=K_P e_f+K_D \frac{def}{dT} +P_{INV} \qquad (4)$$

The derivative part of the PD regulator increases the system speed response and stability. The PD proportional part makes the BESS increases the system load when the frequency is above the rated value ($e_f > 0$) and, conversely, the BESS generates power when the frequency is below the rated value ($e_f < 0$). This is a kind of a droop speed control, which adds stability and improves the system transients. This PD control is also compatible with the DE isochronous speed control, which is of Proportional–Integral- Derivative (PID) type, as only the integral actuation of the diesel PID corrects the steady state frequency error. The K_P and K_D values are given in the appendix and the exact form of P_{INV} is shown in the next section. Finally the sensor node N_W with the periodic message shown in Fig. 4.1.

3.1. DISTRIBUTED CONTROL SYSTEM

DOI: 10.18535/ijecs/v5i4.16

Generally, the concept of automatic control includes accomplishing two major operations; the transmission of signals (information flow) back and forth and the calculation of control actions (decision making). Carrying out these operations in real plant requires a set of hardware and instrumentation that serve as the platform for these tasks. Distributed control system (DCS) is the most modern control platform. It stands as the infrastructure not only for all advanced control strategies but also for the lowliest control system. The idea of control infrastructure is old. The next section discusses how the control platform progressed through time to follow the advancement in control algorithms and instrumentation technologies.

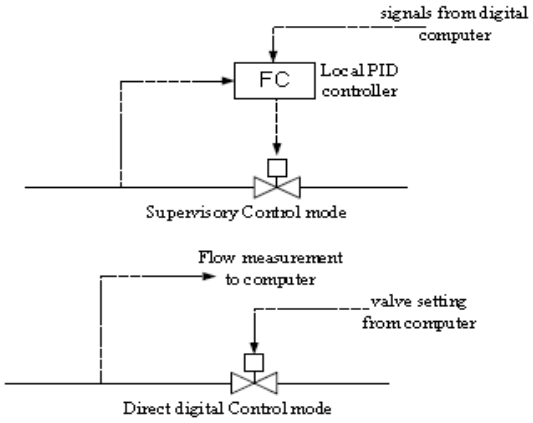

Fig5.1 Computer control modes.

3.1.1. The advantages of DCS systems

The major advantages of functional hardware distribution are flexibility in system design, ease of expansion, reliability, and ease of maintenance. A big advantage compared to a single-computer system is that the user can start out at a low level of investment. Another obvious advantage of this type of distributed architecture is that complete loss of the data highway will not cause complete loss of system capability. Often local units can continue operation with no significant loss of function over moderate or extended periods of time.

Moreover, the DCS network allows different modes of control implementation such as manual/auto/supervisory/computer operation for each local control loop. In the manual mode, the operator manipulates the final control element directly. In the auto mode, the final control element is manipulated automatically through a low-level controller usually a PID. The set point for this control loop is entered by the operator. In the supervisory mode, an advanced digital controller is placed on the top of the low-level controller (Figure 5.1). The advanced controller sets the set point for the low-level controller. The set point for the advanced controller can be set either by the operator or a steady state optimization. In the computer mode, the control system operates in the direct digital mode shown in Figure 5.1.

4. SIMULATION CIRCUITS AND RESULTS

4.1 SIMULATION CIRCUIT AND EXPLANATIONS

The Matlab–Simulink model of the WDHS of Fig.2.1 is shown in Fig. 4.1. Some of the components described next such as the IG, the SM and its voltage regulator, the consumer load, the 3 phase breaker, the elevating transformer, etc. are blocks which belong to the SimPowerSystems library for Simulink.

The DE along with its actuator and speed regulator are included in the Diesel Engine block of Fig. 2 and their modeling is justified. This block has the current SM speed (pu) as input and outputs the mechanical power (pu) to take the DG speed to its 1 pu speed reference. The DE has been simulated by means of a gain, relating fuelling rate to torque, and a dead time, modeling the firing delay between pistons. The DE output torque has a 0 low limit, so the DE braking capability commented in Section 2 is not used, which means considering the worst case in the reverse power situation. The DE output torque high limit is 1.1 pu. The actuator has been simulated by a second order system and the speed regulator by a PID control. The inertia constant of the set DE + SM HDG is 1.75 s.

The sixth order model SM has a rated power ($P_{SM\text{-}NOM}$) of 300 kVA. It receives as input the DE mechanical output power from the DE block. An IEEE type 1 voltage regulator plus an exciter regulates the voltage in the SM terminals. The constant speed stall controlled WTG consists of a fourth order model Induction Generator (IG) of 275 kW (WTG rated power $P_{T\text{-}NOM}$ = 275 kW) directly connected to the autonomous grid and the Wind Turbine (WT) block. This WT block contains the wind turbine characteristic which defines the mechanical torque applied to the IG as a function of the wind speed and the IG shaft speed. This WTG has no pitch control, so there is no way to control the power it produces. The IG consumes reactive power so a 25 kVA capacitor bank has been added to compensate the power factor.

The consumer Load consists of a 175 kW main load and a 125 kW extra load that can be connected–disconnected by closing/opening the 3 Phase Breaker (3PB) of Fig.4.1. The BESS is based on a Ni–Cd battery bank, a LC filter, an IGBT three-phase bidirectional Current Controlled Inverter (CCI) of rated power $P_{S\text{-}NOM}$ = 150 kW and a 150 kVA elevating transformer. The elevating transformer with a transformation ratio of 4 isolates the three phase power inverter and the battery bank from the autonomous grid and allows to use a standard battery bank voltage of 240 V.

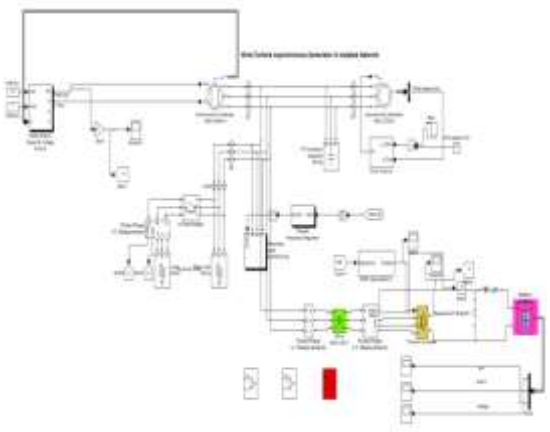

Fig. 4.1 Simulink/SimPowerSystem schematic simulated system.

A detailed description of the CCI block . The CCI receives its active power reference PS-REF from the Active Power Regulator (APR). PS-REF can be established for inverter mode operation (the CCI supplies power to the isolated grid and discharges the battery), or rectifier mode operation, (the CCI absorbs power from the isolated grid and charges the battery).

Although the CCI can control the reactive power it consumes/produces its reactive reference power is set to 0. The 240 V Ni–Cd battery model has been taken from and its Simulink schematic is shown in Fig.4.2 . The model consists of the controlled variable voltage source of value E in series with an internal constant resistance R. E depends on the capacity extracted from the battery R idt (Ah) and the maximum theoretical battery capacity Q (Ah)

(generally equal to 105% of the rated capacity) according to equation (5):

$$E=E_O-K\frac{Q}{Q-\int idt}+A\exp^{(-B\int idt)} \quad (5)$$

The equation parameters E0, K, A and B (values in the appendix) are obtained from the discharge characteristic of the battery. The state of charge (SOC) of the battery is cero when the battery is empty and 100% when is fully charged and is calculated as:

$$SOC=100\left(1-\frac{1}{Q}\int idt\right) \quad (6)$$

The model in does not vary with the temperature, assumes the same parameters for charging and also that the capacity of the battery does no change with the amplitude of the current. On the other hand a storage energy need of 15 min for the 150 kW CCI rated power and a Ni–Cd battery operating between 35% and 75% of its rated capacity gives 93.75 kWh as the energy stored in the battery (150 kW _ 15 min/(0.4 _ 60 min/h) = 93.75 kWh) . This battery sizing is justified in to minimize the number of the DGs start/stop cycles needed in order to reduce the fuel consumption and DGs wearing. This 93.75 kWh corresponds, as the battery rated voltage is 240 V, to a rated capacity C of 390.625 Ah (93.75 kWh/240 V = 390.625 Ah), so Q takes the value of 410.16 Ah. The Ni–Cd battery is tolerant to a current ripple of rms value up to 0.2⁄C with the only effect of an increased water usage . Connecting the battery directly to the DC side of the power converter would excess this ripple size, so a LC filter has been used for smoothing the battery current. Considering the 390.625 Ah battery rated capacity, an rms ripple current up to 78 A would be permissible. Using formulas from values for the electrolytic capacitor, 8 mF, and for the inductor, 2.5 lH, were calculated to obtain an rms ripple under 0.04⁄C (15.6 A), that is five times less than the previous requirement. Although in the simulation section ahead, the BESS is used to increase the system load so that the DG reverse power is avoided, the BESS when acting as a source helps to cover the load during short term load peaks or wind power deficits . Also short term BESS improves the frequency stability .

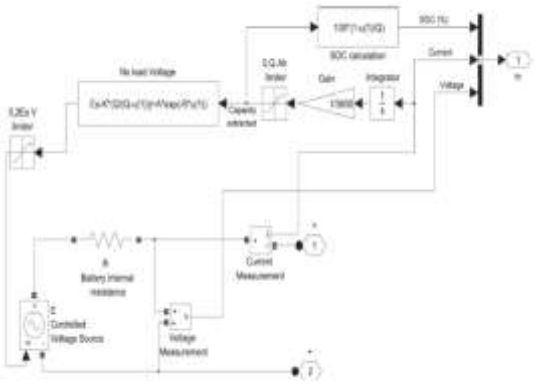

Fig. 4.2 Ni–Cd Battery Simulink schematic.

The N_W node of Fig. 2.1 is simulated by APR block of Fig. 4.1. The APR receives as inputs the shaft speed and active power of the SM. It outputs P_{REF} according to (4) to the CCI block. The APR schematic is shown in Fig. 4 and applies a discrete PD control to the frequency error with a 2.5 ms sample time. This 2.5 ms sample time sets the 400 Hz transmission frequency for the P_{REF} message of Fig.2.1.

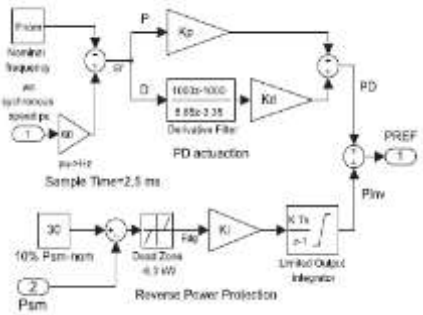

Fig. 4.3 APR Simulink schematic

The proportional and derivative constants K_P and K_D respectively (values in Appendix), has been chosen to position the dominant pole pair of the WDHS linearized model to be a double pole in order to increase the speed of response, reducing the settling time and minimizing the system frequency over/under shooting. Instead of a pure derivative block, the lead compensator of Fig. 4.3 has been used. In Fig. 4.3 is also shown the diagram of the reverse

DOI: 10.18535/ijecs/v5i4.16

power protection control. This controller is a simple integral control with the P_{SM} as input, the 30 kW P_{DG-MIN} minimum SM power as reference (10% of P_{SM-NOM}) and the power to be consumed by the BESS as output (P_{INV}). The dead zone, starting at _6 kW and ending at 0 kW (2% of P_{SM-NOM}), implements an offset to avoid excessive action of this protective control. According to Fig. 4.3, P_{INV} increases (with a P_{S-NOM} higher limit) when PSM < 30 kW ($e_{DG} > 0$), decreases (with a 0 lower limit) when $P_{SM} > 36$ kW ($e_{DG} < 0$) and PSM in the range from 30 to 36 kW ($e_{DG} = 0$) results in zero dead zone output and keeps P_{INV} constant. Therefore when this protection is activated steady state DG power is kept in the range from 30 to 36 kW.

4.2 SIMULATION RESULTS

In this section graphs for the following variables are shown: the frequency per unit (fpu) (Fig. 4.4), the RMS voltage per unit (Fig. 4.5), the active powers for the WTG and DG (Fig. 4.6), the active powers for consumer load and BESS (Fig. 4.7) and the battery voltage–current– SOC (Fig. 4.8). For the WTG and DG (Fig. 4.6) the active powers are considered positive if produced and for the load and BESS positive if consumed, so that the same sign criteria of equations (1)-(3) is used. At the test starting point the wind speed is 10 m/s, the WTG and DG are producing active powers of 199 kW and 101 kW respectively, the load and BESS are consuming active powers of 300 kW (3PB is closed) and 0 kW respectively and the battery SOC is 50%, being the system in equilibrium. At t = 0.2 s a 125 kW negative load step is applied by opening the 3PB of Fig. 2 reducing the total consumer load to 175 kW, which is less than the previous WTG produced active power (199 kW). The DG reacts by decreasing its generated power and when it is below 30 kW the DG reverse power protection is activated. This protection increases the power consumed by the BESS so that in steady state the DG produced power falls within the 30–36 kW DG minimum power interval. The transient finishes at t = 7.67 s with WTG producing the same 199 kW previous to the negative load step as the wind speed has not changed, the DG producing 32 kW (a value in the 10–12% PSM-NOM range) and the BESS consuming 56 kW. During this _125 kW load step the frequency and voltage minimum/maximum are 0.9982/1.0078 pu and 0.9829/1.0072 pu respectively and the frequency shows undershooting due to the integral actuation of reverse power protection. The system frequency response without the BESS actuation (no BESS consumption) is plotted in using a dashed style. Fig. 2.4 shows that in the no BESS actuation case it is necessary to open the WTG circuit breaker to avoid the over speed alarm and the collapse of the power system.

At t = 8.2 s the wind speed changes from its initial value of 10 to 7 m/s. In Fig.4.6 it is shown that the power of WTG is decreased from its initial 199 kW value to 50 kW in steady state. Figs. 7 and 8 also present brief oscillations in the WTG, DG, BESS and load active powers after the negative wind step. The variations in the power consumed by the load are due to the voltage variations since the load is purely resistive. During this _3 m/s wind step the minimum–maximum voltages are 0.9814/1.0179 pu and Fig. 4.4 shows a no overshooting fpu with minimum–maximum values of 0.9933/1.0001 pu. In steady state reached at t = 13.12 s the active powers for the WTG and DG are 50 kW and 125 kW respectively and 0 for the BESS as the load power (175 kW) is less than the WTG power, so that the BESS is not needed to avoid a DG reverse power.

The Battery SOC, voltage normalized to its 240 V rated voltage, and current normalized to its 625 A rated current (150 kW/ 240 V = 625 A) are shown in Fig. 4.8. The battery current is considered positive if the battery is charging and negative if discharging.

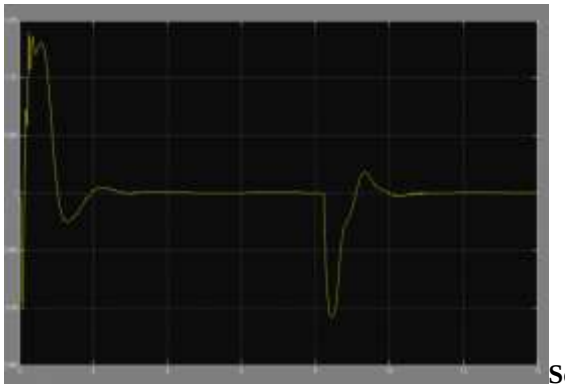

Screen 4.1 Frequency per unit

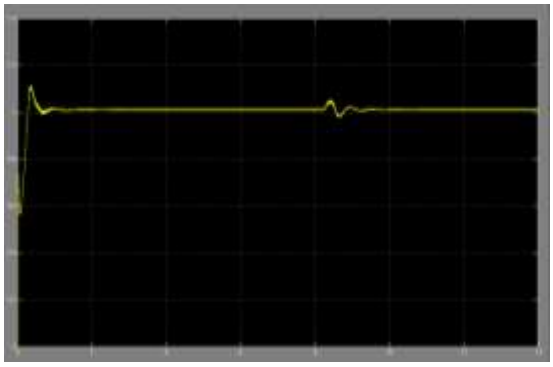

Screen 4.2 RMS voltage per unit

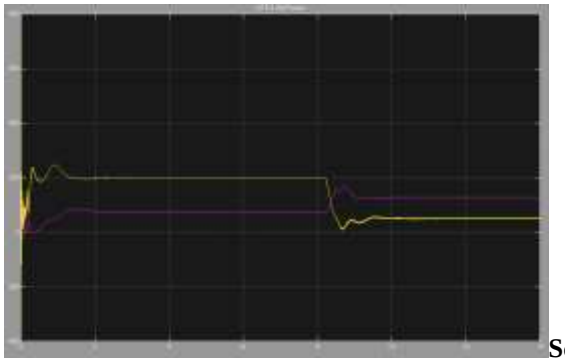

Screen 4.3 Generated(+) active powers by the WTG and DG.

As it can be seen in Fig. 4.8, the battery current resembles a scaled version of the BESS active power in Fig. 4.7, due to the almost constant value of the battery voltage during the simulation. During the _125 kW load step the battery is charged being the current peak 0.419 pu and the steady state current 0.352 pu.

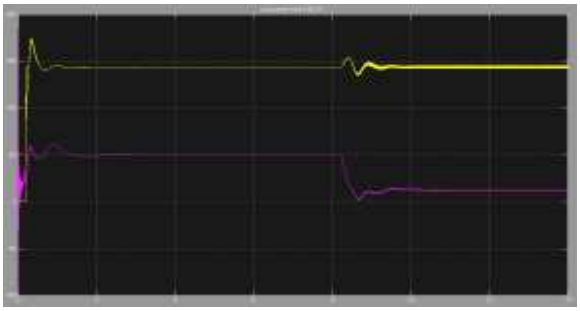

Screen 4.4 Consumed (+) active powers by the BESS and load.

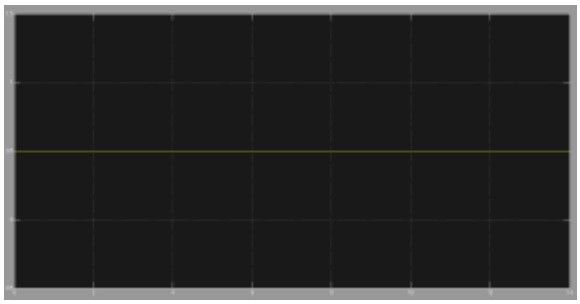

Screen 4.5. Normalised battery SOC

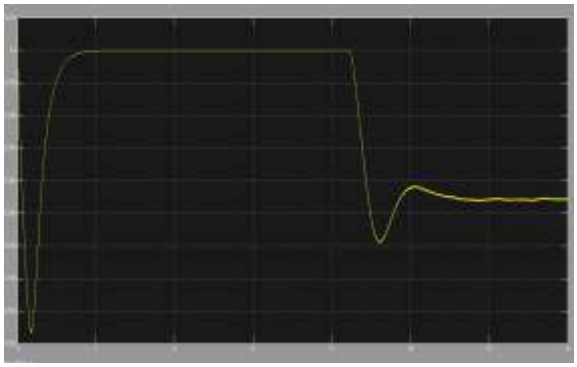

Screen 4.6. Normalized battery voltage

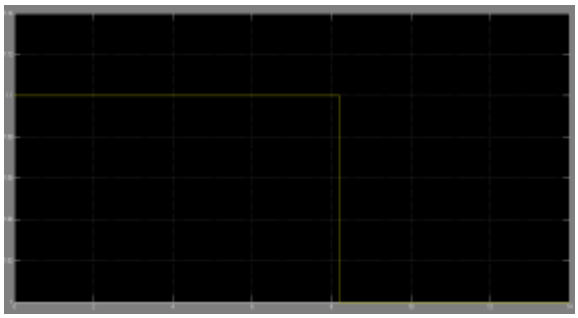

Screen 4.7 Normalized battery current.

Also it can be seen a current ripple which increases with the mean current value, being 3A rms in steady state. This 3A rms value is less than the 15.6 A (0.04⁄C) rms ripple design requirement established in Section 4. During the _3 m/s wind step the current peak is _0.387 pu and the steady state value is 0 since the BESS is not needed when the system reaches the equilibrium. The battery SOC initially set at 50%, barely changes due to the short simulation time and its relatively great capacity. The variations of the normalized battery voltage are small from 1.024 to 1.056 pu during the test. These variations follow the current variations due to the internal battery resistance since SOC variations are negligible. The lowest voltage is due to the negative peak current after the _3 m/s wind step. The highest voltage is due to positive peak current after the _125 kW step.

CONCLUSION

The WDHS Simulink model has been presented and tested for consumer load and wind speed changes. The negative load step leads the system to a DG reverse power and it has been shown how the control system by an integral action increases the BESS load until the DG power falls in a minimum predetermined power interval.

The negative wind step decreases the WTG produced power, returning the power system to a situation where the WTG power is less than the consumer load power, so that the BESS is not needed to load artificially the system. In both steps the PD regulator makes the BESS to filter the fluctuations of the wind power as wells as those of the consumer loads, improving effectively the transients of the WDHS.

REFERENCES

[1] Wind/Diesel Systems Architecture Guidebook. American Wind Energy Association;1991.

[2] Drouilhet S. High penetration AC bus wind-diesel hybrid power systems. Village Power´ 98, Technical workshop, Washington DC; October 1998.

[3] Hunter R, Infield D, Kessler S, de Bonte J, Toftevaag T, Sherwin B, et al. Designing system. In: Hunter R, Eliot G, editors. Wind-diesel systems: a guide to the technology and its implementations. Cambridge, UK: Cambridge University Press

[4] Muljadi E, McKenna HE. Power quality issues in a hybrid power system. IEEE Trans Ind Appl 2002;38(3):803–9.

[5] Sedaghat B, Jalilvand A, Noroozian R. Design of a multilevel control strategy for integration of stand-alone wind/diesel system. Int J Electr Power Energy Syst 2012;35(1):123–37.

[6] Sebastian R. Modelling and simulation of a high penetration wind diesel system with battery energy storage. Int J Electr Power Energy Syst 2011;33(3):76774.http://dx.doi.org/10.1016/j.ijepes.2010.12.034, ISSN0142-0615.

[7] Sebastián R, Peña Alzola R. Effective active power control of a high penetration wind diesel system with a Ni–Cd battery energy storage. Renew Energy 2010;35(5):952–65. http://dx.doi.org/10.1016/j.renene.2009.11.02. ISSN 0960-1481.

[8] Sebastián R, Peña Alzola R. Simulation of an isolated wind diesel system with batteryenergy storage. Electr Power Syst Res 2011;81(2):677–86.

[9] Elkhatib Kamal, Magdy Koutb, Abdul Azim Sobaih, Belal Abozalam. An intelligent maximum power extraction algorithm for hybrid wind-dieselstorage system. Int J Electr Power Energy Syst 2010;32(3):170–7.

http://dx.doi.org/10.1016/j.ijepes.2009.07.005. ISSN 0142-061.
[10] Du W, Wang HF, Cheng S, Wen JY, Dunn R. Robustness of damping control implemented by energy storage systems installed in power systems. Int JElectr Power Energy Syst 2011;33(1):35–42. doi: 10.1016/j.ijepes.2010.08.006, ISSN: 0142-0615.

AUTHORS

C.MD.SHAREEF working as Asst Prof., in Vemu Institute of Technology, P.Kothakota. He completed his mtech in the stream of Electrical Power Systems. He has 6years of teaching experience. His area of interest is on High Voltage DC Transmission and FACTS Controllers.

RAJASEKAR THOTA, working as Asst Prof., in Vemu Institute of Technology, P.Kothakota., JNTU,anantapuram. He completed his mtech in the stream of Electrical Power Systems. He has 3years of teaching experience. His area of interest is on Power System Quality and Relibility issues and mainly on Renewable Energy Sources.

N VASEEM RAJA, working as Asst Prof., in Vemu Institute of Technology, P.Kothakota., affiliated to JNTUA,anantapuramu. He completed his mtech in the stream of Electrical Power Systems. His area of interest is on High Voltage Engineering and Power Quality Issues.

T.NARASIMHA REDDY, working as Asst. Professor in Vemu Institute of Technology, p.kothakota., affiliated to JNTUA,Anantapuramu. He completed his MTech in the stream of Electrical Power Engineering SITAMS chittoor., affiliated to JNTUA,Anantapuramu. His area of interest is on Power System reliability.